Dynamics of Atmospheres and Oceans 75 (2016) 33–45

Contents lists available at ScienceDirect

Dynamics of Atmospheres and Oceans

journal homepage: www.elsevier.com/locate/dynatmoce

Subseasonal variability and predictability of the Arctic Oscillation/North Atlantic Oscillation in BCC_AGCM2.2

Jinqing Zuo[a,b], Hong-Li Ren[a,c,*], Jie Wu[a,b], Yu Nie[a], Qiaoping Li[a]

[a] Laboratory for Climate Studies & CMA-NJU Joint Laboratory for Climate Prediction Studies, National Climate Center, China Meteorological Administration, Beijing 100081, China
[b] Collaborative Innovation Center on Forecast and Evaluation of Meteorological Disasters, Nanjing University of Information Science & Technology, Nanjing 210044, China
[c] Joint Center for Global Change Studies (JCGCS), Beijing 100875, China

ARTICLE INFO

Article history:
Received 18 January 2016
Received in revised form 25 March 2016
Accepted 12 May 2016
Available online 13 May 2016

Keywords:
Subseasonal AO/NAO variability
Predictability
Storm track activity
Synoptic eddy feedback
Troposphere–stratosphere coupling

ABSTRACT

The subseasonal variability and predictability of the Arctic Oscillation/North Atlantic Oscillation (AO/NAO) is evaluated using a full set of hindcasts generated from the Beijing Climate Center Atmospheric General Circulation Model version 2.2 (BCC_AGCM2.2). It is shown that the predictability of the monthly mean AO/NAO index varies seasonally, with the highest predictability during winter (December–March) and the lowest during autumn (August–November), with respect to both observations and BCC_AGCM2.2 results. As compared with the persistence prediction skill of observations, the model skillfully predicts the monthly mean AO/NAO index with a one-pentad lead time during all winter months, and with a lead time of up to two pentads in December and January. During winter, BCC_AGCM2.2 exhibits an acceptable skill in predicting the daily AO/NAO index of ~9 days, which is higher than the persistence prediction skill of observations of ~4 days. Further analysis suggests that improvements in the simulation of storm track activity, synoptic eddy feedback, and troposphere–stratosphere coupling in the Northern Hemisphere could help to improve the prediction skill of subseasonal AO/NAO variability by BCC_AGCM2.2 during winter. In particular, BCC_AGCM2.2 underestimates storm track activity intensity but overestimates troposphere–stratosphere coupling, as compared with observations, thus providing a clue to further improvements in model performance.

1. Introduction

The North Atlantic Oscillation (NAO) is the dominant mode of atmospheric low-frequency variability in the North Atlantic sector (Hurrell et al., 2003; Li and Wang, 2003). The NAO is generally considered to be a regional manifestation of the hemispheric-scale Arctic Oscillation (AO) during winter, which is also known as the Northern Annular Mode (NAM; Thompson and Wallace, 1998, 2000; Wallace, 2000). Many studies have demonstrated that changes in the polarity of the AO/NAO tend to be accompanied by large-scale weather and climate anomalies on the northern continents during winter (Thompson and Wallace, 1998, 2001; Hurrell et al., 2003; Zuo et al., 2015 and references therein). Therefore, the skillful prediction of the AO/NAO variability at subseasonal–seasonal (S2S) timescales is of great importance.

* Corresponding author at: Laboratory for Climate Studies & CMA-NJU Joint Laboratory for Climate Prediction Studies, National Climate Center, China Meteorological Administration, Beijing 100081, China.
E-mail address: renhl@cma.gov.cn (H.-L. Ren).

http://dx.doi.org/10.1016/j.dynatmoce.2016.05.002

Sub-seasonal to interannual variability of the AO/NAO is generally dominated by atmospheric internal dynamics (Yamazaki and Shinya, 1999; Feldstein, 2000; Robertson, 2001; Hurrell et al., 2003). Due to the chaotic nature of atmospheric dynamics, skillful prediction of the AO/NAO variability at S2S timescales will be challenging. In the early 21th century, a majority of the climate models showed a fairly low prediction skill of the winter-mean AO/NAO index (Doblas-Reyes et al., 2003; Müller et al., 2005; Johansson, 2007; Arribas et al., 2011; Qian et al., 2011; Kim et al., 2012). Recent studies demonstrated that several state-of-the-art seasonal model forecast systems have shown significant improvements in predicting the winter-mean AO/NAO index, with lead times of up to 2 months (Riddle et al., 2013; Kang et al., 2014; Scaife et al., 2014; Sun and Ahn, 2015).

These studies mainly focused on the seasonal predictability of the AO/NAO in climate models. However, studies focusing on the subseasonal prediction skill of the AO/NAO index are rare. Johansson (2007) assessed the skill of hindcasts at predicting the NAO index using two operational dynamical forecast systems, one from the National Centers for Environmental Prediction (NCEP) and the other from the European Centre for Medium-Range Weather Forecasts (ECMWF). They noted that the prediction skill of the hindcasts with respect to the NAO was negligible at subseasonal timescales. Vitart (2014) recently demonstrated that the annual skill scores of the ECMWF reforecast in predicting subseasonal variability of the NAO had evidently improved from 2002 to 2012, and specifically, that the NAO at week 2–3 in winter is reasonably predictable.

Previous studies have suggested that at subseasonal timescales, a potential source of predictability of the AO/NAO likely originates in the Madden–Julian Oscillation (MJO) (Zhou and Miller, 2005; Cassou, 2008; L'Heureux and Higgins, 2008; Lin et al., 2009). Through downward propagation of the westerly and easterly anomalies, the weakened polar vortex in the Northern Hemisphere stratosphere tends to be followed by a negative phase of the AO/NAO in the troposphere and near-surface during winter (Baldwin and Dunkerton, 2001; Baldwin et al., 2003; Norton, 2003; Scaife et al., 2005; Wang and Chen, 2010). This suggests that variations in the stratospheric polar vortex may also provide an important source of predictability of the AO/NAO at S2S timescales (Maycock et al., 2011; Gerber et al., 2012 and references therein). Some studies have demonstrated that subseasonal AO/NAO predictions during winter can be improved by increasing the accuracy of the representations of both the MJO (Vitart, 2014) and stratospheric polar vortex signals (Sigmond et al., 2013; Tripathi et al., 2015) in the initial conditions of the model.

Observed and numerical studies have revealed that interaction between low-frequency flow and synoptic eddy plays an indispensable role in maintaining or enhancing the AO/NAO variability (e.g., Lorenz and Hartmann, 2003; Jin et al., 2006a, 2006b; Ren et al., 2009, 2012, 2014; Tan et al., 2014). Since synoptic eddy feedback is of great importance for maintaining or enhancing low-frequency variability, it is clearly indicated that model performance in simulating such an feedback is crucial to reasonably reproduce the AO/NAO variability at S2S timescales. This is supported by Kang et al. (2011) which noted a remarkable impact of synoptic eddy feedback on extratropical seasonal-mean predictability in DEMETER models.

This study aims to evaluate the skill of the Beijing Climate Center Atmospheric General Circulation Model version 2.2 (BCC_AGCM2.2) in predicting subseasonal AO/NAO variability, using a set of hindcasts generated from this model. More importantly, we investigate deficiencies of the model in simulating the AO/NAO pattern and related atmospheric mechanisms for maintaining the pattern. BCC_AGCM2.2 has been shown to perform reasonably in simulating the mean state of global precipitation (Wu et al., 2014).

The remainder of this paper is organized as follows. Section 2 introduces the model, data, and methods. Section 3 presents skill scores of BCC_AGCM2.2 in predicting monthly and daily AO/NAO indices. Section 4 examines the performance of the model in simulating the spatial pattern of the winter-time AO/NAO, and considers related mechanisms for maintaining the pattern involving synoptic eddy feedback and troposphere–stratosphere coupling, while MJO's impact on the subseasonal variability of the AO/NAO is addressed in Wu et al. (2016, under review). Finally, Section 5 provides a summary and discussion.

2. Model, data, and methodology

2.1. Hindcast and reanalysis

The BCC_AGCM2.2 has a horizontal resolution of T106 and includes 26 vertical levels (Wu et al., 2014). The top of the model is at 2.3 hPa. The model is initialized using the atmospheric conditions from the NCEP Reanalysis dataset (Kalnay et al., 1996) and sea-surface conditions from NOAA Optimum Interpolation Sea Surface Temperature V2 (Reynolds et al., 2002). Four model runs (00Z, 06Z, 12Z, and 18Z) are initialized every day starting on 1 January 1983 and run for 55 days each. Daily mean is generated as the ensemble average of all the four members. Daily and monthly averaged outputs are used. The model output is interpolated to a $2.5^\circ \times 2.5^\circ$ horizontal resolution prior to analysis. To verify the model hindcast, we use the daily and monthly ERA-Interim dataset for the period 1983–2013 (Dee et al., 2011). These data have a horizontal resolution of $2.5^\circ \times 2.5^\circ$. The winter mean is generated as the average of December–January–February values.

2.2. Calculations of indices and prediction skill

We define the AO as the first leading empirical orthogonal function (EOF1) pattern of area-weighted monthly mean sea level pressure (SLP) anomalies north of 20°N (Thompson and Wallace, 2000) and the NAO as the EOF1 of area-weighted monthly mean SLP anomalies over the North Atlantic sector (80°W–40°E, 20°N–90°N) (Hurrell et al., 2003) during 1984–2013. The monthly and daily AO/NAO indices are calculated as the projection onto the AO/NAO loading pattern. Sim-

ilarly, the stratospheric polar vortex (SPV) index is calculated as the projection onto the EOF1 of area-weighted monthly mean 50 hPa geopotential height anomalies north of 20°N (Baldwin and Dunkerton, 2001).

The prediction skill of BCC_AGCM2.2 with respect to the AO/NAO is evaluated using temporal correlation coefficients between predicted and observed AO/NAO indices. Here, the observed AO/NAO index is calculated using the ERA-Interim SLP anomalies, and the predicted index is calculated as the projection of the model prediction onto the observed AO/NAO pattern. The persistence prediction provides a baseline for verification, and the dynamical prediction skill is considered to be useful only when it exceeds that of the persistence prediction. For the monthly timescale, the persistence prediction skill is calculated as the 1 month lagged autocorrelation of the observed index.

2.3. Calculations of storm track activity intensity and synoptic eddy feedback

Storm track activity intensity is calculated as the root mean square of the synoptic-eddy component of the daily geopotential height at 300 hPa. Following Chang and Fu (2002), we apply a 24 h difference filter to the daily time series to obtain the associated synoptic-eddy component. According to the quasi-geostrophic potential vorticity equation, the synoptic eddy-vorticity feedback to the anomalous low-frequency flow can be depicted by a stream function tendency (ψ^t) satisfying the following relationship (Lau and Holopainen, 1984):

$$\psi^t = -\nabla^{-2}\left(\nabla \times \overline{V'\zeta'}\right), \quad (1)$$

where V and ζ are the horizontal wind vector and relative vorticity, respectively, the prime represents the synoptic-eddy component, and the overbar denotes a time average. The stream function tendency due to synoptic eddy-vorticity forcing is obtained by solving Poisson's equation.

3. Prediction skill of BCC_AGCM2.2 with respect to the AO/NAO

Fig. 1 shows the prediction skill of BCC_AGCM2.2 with respect to monthly AO and NAO indices for the period 1984–2013. The results show that seasonal variations in the correlation skill of the monthly AO index resemble those of the monthly NAO index, in both BCC_AGCM2.2 and observations. Specifically, the AO and NAO indices both exhibit the highest predictability during winter (December–March) and the lowest predictability during autumn (August–November). As compared with observations, BCC_AGCM2.2 tends to exhibit a higher skill in predicting the monthly AO/NAO index with lead times of up to one pentad for all calendar months, except for July. It is interesting to see that the persistence skill of observations and predication skill of model hindcasts are both relatively high in July, which deserves a further study in future. For the winter months, when the AO/NAO index exhibits the highest predictability, the prediction skills of the monthly AO and NAO indices are almost higher than 0.7 (0.6) at zero- (one-) pentad lead in the model, which are obviously higher than the persistence prediction skill. With a lead time of two pentads, BCC_AGCM2.2 shows skillful prediction of the AO and NAO indices only in December and January.

Fig. 2a further shows the skill of the model at predicting the daily AO and NAO indices as a function of lead times during winter. The skill at predicting the daily NAO index is nearly equivalent to that of the daily AO index, and decreases with increasing lead time in both BCC_AGCM2.2 and observations. Assuming that a correlation coefficient of 0.5 or above represents an acceptable level of prediction of the AO/NAO by BCC_AGCM2.2, the model shows a skill of ~9 days in predicting the AO and NAO indices, which is significantly higher than the persistence prediction skill of observations of ~4 days. At pentad timescale, the model exhibits a prediction skill of only about one pentad in predicting the AO/NAO index during winter (Fig. 2b).

4. Model diagnostics

Our results indicate that the skill of BCC_AGCM2.2 at predicting the AO/NAO index at daily to monthly timescales during winter is greater than that of the persistence skill of observations. The potential sources of predictability in BCC_AGCM2.2 may be related to several factors, including model dynamics, physical processes, and initial conditions; however, a full investigation of these sources of predictability is beyond the scope of this study. This section focuses specifically on the performance of the model in simulating spatial patterns of the AO/NAO, mechanisms of synoptic eddy feedback that help maintain the pattern, and the impacts of stratospheric initial conditions on the skill at predicting the AO/NAO during winter.

4.1. AO/NAO pattern

Fig. 3 shows the spatial pattern of the AO/NAO, represented as regressions of SLP anomalies on the AO/NAO index, as derived from both observations and the BCC_AGCM2.2 hindcasts, at zero- to two-pentad lead times during winter. The NAO pattern strongly resembles the AO pattern in both observations and BCC_AGCM2.2. The model performs well at capturing the spatial pattern of the AO/NAO, exhibiting a spatial correlation coefficient between the observed and simulated patterns of $\geq$0.92 (Table 1).

However, the explained variance of the AO pattern in BCC_AGCM2.2 of 33%–36% is greater than that of observations (~21%) (Table 1). This is also true for the explained variance of the NAO pattern. Moreover, the amplitude of the AO/NAO pattern as

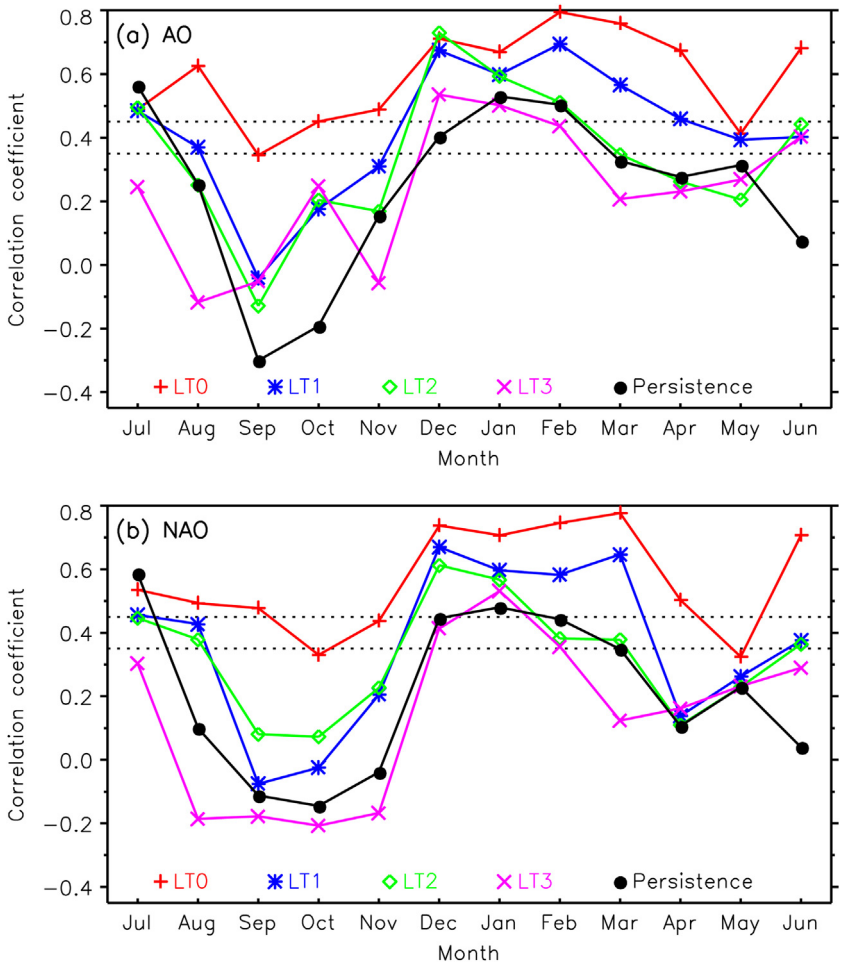

Fig. 1. Persistence skill of observations (black lines) and predication skills of model hindcasts (colored lines, representing lead times, LT, of zero to three pentads) at forecasting the monthly (a) AO and (b) NAO indices, as measured by the correlation coefficient between observed and predicted indices. Dashed lines denote significance at the 95% (lower) and 99% (upper) confidence levels.

Table 1
Percentages of explained variance (unit: %) of the AO and NAO patterns in observation (OBS) and model hindcasts, standard deviations of the patterns normalized by observations, spatial correlations between observed and simulated patterns, and temporal correlations of the AO index with the NAO and stratospheric polar vortex (SPV) indices. LT denotes the lead time (pentads).

			Hindcasts			
		OBS	LT = 0	LT = 1	LT = 2	LT = 3
AO pattern	Explained variance	20.9	34.4	33.4	36.2	34.9
	Standard deviation	/	1.00	0.81	0.74	0.74
	Spatial correlation	/	0.96	0.95	0.93	0.92
NAO pattern	Explained variance	37.0	47.9	49.8	52.4	53.5
	Standard deviation	/	0.82	0.65	0.57	0.52
	Spatial correlation	/	0.97	0.96	0.96	0.96
Temporal correlation (AO, NAO)		0.95	0.97	0.96	0.95	0.97
Temporal correlation (AO, SPV)		0.58	0.82	0.87	0.88	0.84

predicted by BCC_AGCM2.2 appears to decrease with increasing lead time, with the exception in the North Pacific. Notably, the Arctic activity center of the AO/NAO is located mainly in the North Atlantic in observations; however, in BCC_AGCM2.2 the center is located in the Eurasian sector at lead times of zero to one pentad, and is located mainly in the Arctic at a lead time of two pentads.

The winter-mean NAO index is strongly correlated with the winter-mean AO index (correlation coefficient of $\geq$0.95) in both observations and BCC_AGCM2.2 (Table 1). Because of the high correlation between the AO and NAO indices during winter, we mainly show the results associated with the AO index in the following subsection.

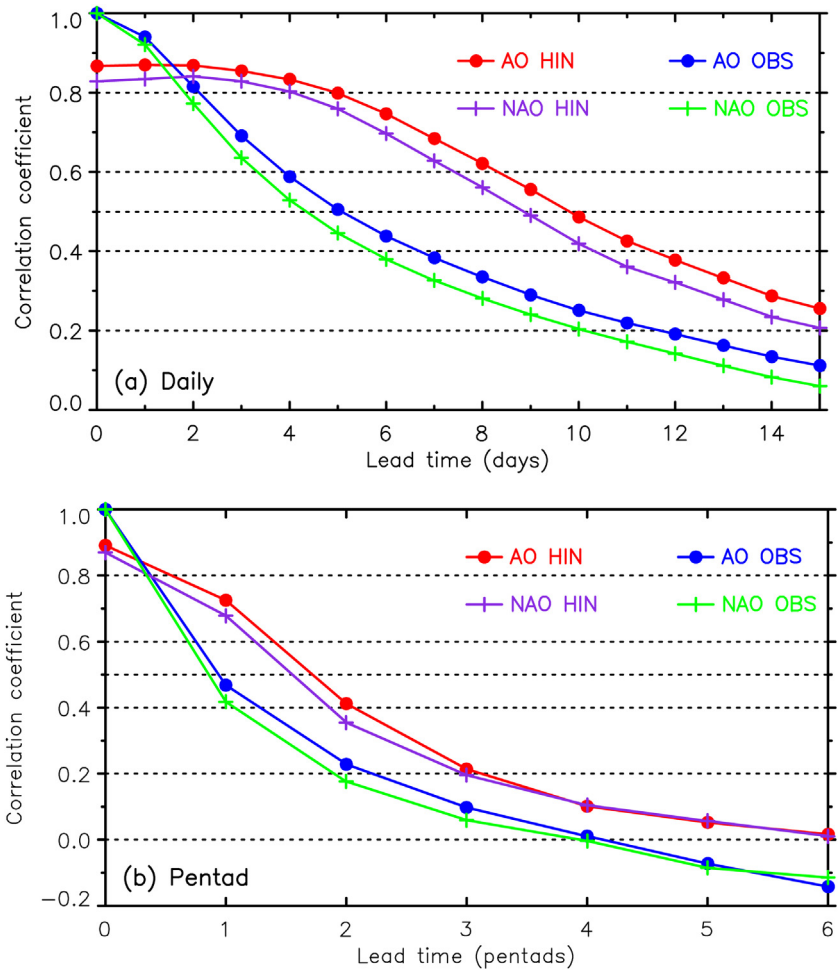

Fig. 2. Skill of the model at forecasting the (a) daily and (b) pentad-scale AO and NAO indices as a function of lead time during winter. The red (purple) line indicates the skill of model hindcasts in predicting the AO (NAO) index, and the blue (green) line refers to the persistence forecast of observations of the AO (NAO) index.

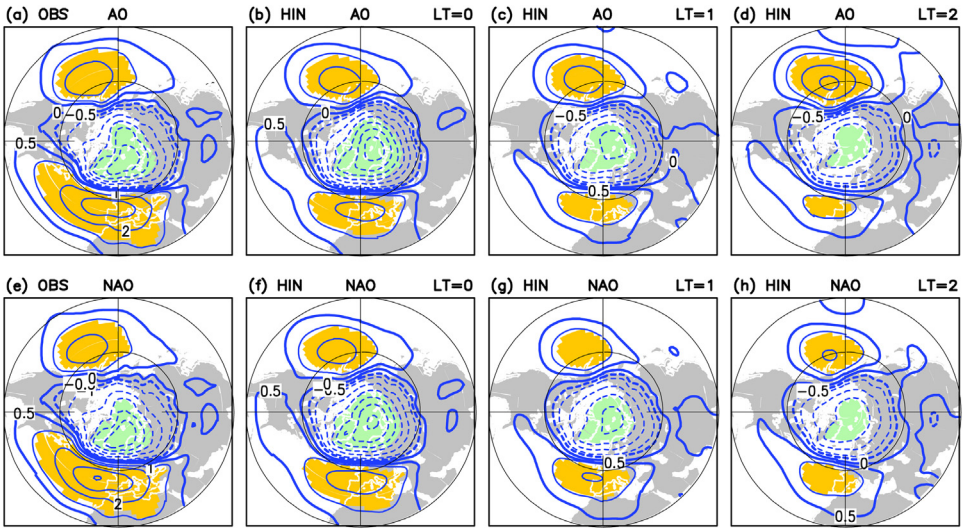

Fig. 3. Spatial patterns of the AO represented as regressions of sea level pressure anomalies (unit: hPa) against the AO index in (a) observations and (b–d) model hindcasts at lead times of zero to two pentads during winter. (e–h) As in (a–d), but for the NAO pattern. Yellow shading indicates regions with regression coefficients greater than 1, and green shading less than −3.

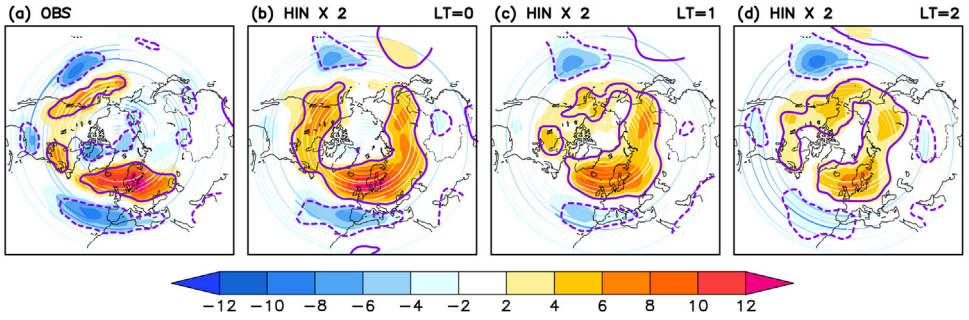

Fig. 4. Regressions of storm track activity anomalies (unit: gpm) at 300 hPa against the AO index in (a) observations and (b–d) model hindcasts at lead times of zero to two pentads during winter. Regions inside the contours are significant at the 95% confidence level. Values in (b–d) have been multiplied by a factor of 2 to facilitate comparison.

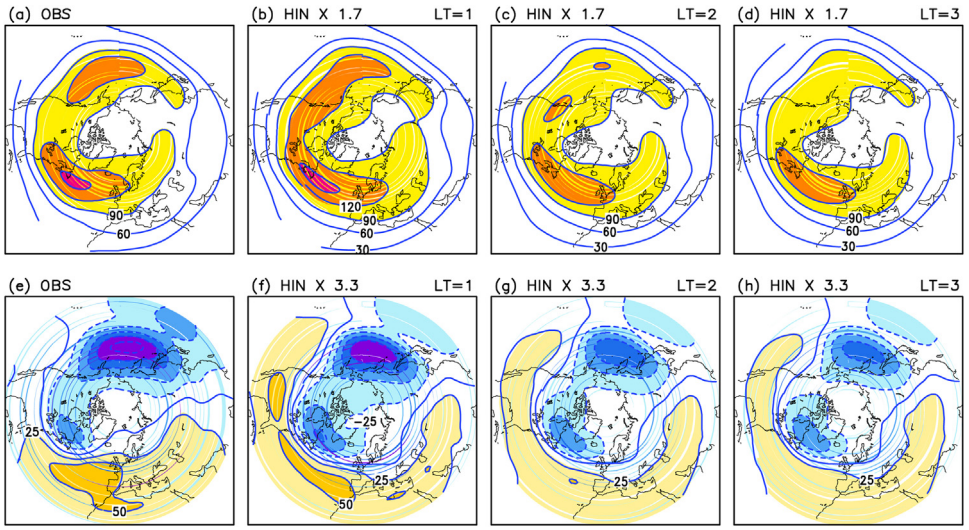

Fig. 5. Climatological mean of storm track activity (unit: gpm) at 300 hPa in (a) observations and (b–d) model hindcasts at lead times of zero to two pentads during winter. (e–h) As in (a–d), but for the stream function tendency (unit: $m^2\ s^{-2}$) due to synoptic eddy-vorticity forcing. Values in (b–d) and (f–h) have been multiplied by a factor of 2 and 3.3, respectively, to facilitate comparisons.

4.2. AO/NAO-associated storm track activity and synoptic eddy feedback

Previous studies have demonstrated that changes in the polarity of the NAO/AO are closely related to changes in the positions of storm tracks and associated synoptic eddy activity over middle latitudes of the Northern Hemisphere during winter (e.g., Hurrell, 1995; Ren et al., 2009). The atmospheric low-frequency mode can be enhanced and maintained by positive feedbacks associated with synoptic eddy activity (Lau and Nath, 1991; Branstator, 1992; Lorenz and Hartmann, 2003). Thus, we tested the ability of BCC_AGCM2.2 to simulate the relationship between the AO/NAO and Northern Hemispheric storm track activity.

Fig. 4 shows storm track activity anomalies regressed onto the AO index in both observations and the BCC_AGCM2.2 hindcasts at zero- to two-pentad lead times during winter. As compared with observations (Fig. 4a), the model provides a good prediction of the pattern of AO-related storm track activity anomalies over the North Atlantic and North Pacific sectors, but significantly underestimates the amplitudes of these anomalies (Figs. 4b–d). Such an underestimate is attributed mainly to evidently weaker amplitudes of storm track activity generated by BCC_AGCM2.2 (Fig. 5). We found that the amplitude of storm track activity in the BCC_AGCM2.2 hindcast at a zero-pentad lead time is only ~60% of the observational value (Fig. 5). In addition, the AO exhibits a strong in-phase relationship with synoptic eddy activity over northern Eurasia in the BCC_AGCM2.2 hindcast (Figs. 4b–d), but such a relationship does not occur in observations (Fig. 4a). This finding indicates that AO-associated changes in synoptic eddy activity over northern Eurasia are overestimated by BCC_AGCM2.2, which is consistent with the eastward shift of the Arctic activity center of the AO predicted by the model.

We further examined the predictions of BCC_AGCM2.2 of the positive feedback of synoptic eddy activity on AO-associated atmospheric low-frequency variability. Observational evidence shows that cyclonic (anticyclonic) stream function tendencies due to synoptic eddy-vorticity forcing at 300 hPa occur over high (middle) latitudes of the Northern Hemisphere (Fig. 6e), which is consistent with the cyclonic (anticyclonic) seasonal-mean stream function anomalies over these regions during pos-

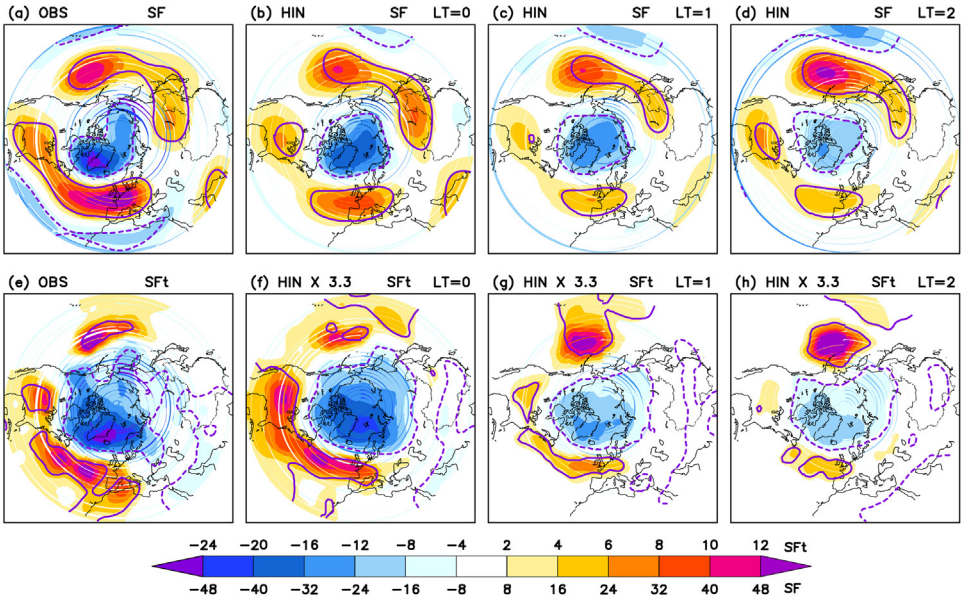

Fig. 6. As in Fig. 4, but for the (a–d) stream function anomalies (unit: $10^5\ m^2\ s^{-1}$) and (e–h) stream function tendency (unit: $m^2\ s^{-2}$) due to synoptic eddy-vorticity forcing at 300 hPa. Values in (f–h) have been multiplied by a factor of 3.3 to facilitate comparisons.

itive phases of the AO (Fig. 6a). This result suggests that synoptic eddy activity plays a role in enhancing and maintaining the AO/NAO pattern, which is in agreement with previous studies (e.g., Kug et al., 2010; Ren et al., 2011, 2012). Moreover, the pattern of the AO-related stream function tendency due to synoptic eddy-vorticity forcing resembles that of the anomalous seasonal-mean flow predicted by BCC_AGCM2.2, which is consistent with observations (Fig. 6). However, due to the systematic weakening of storm track activity in the model, the simulated amplitudes of the climatological mean of synoptic eddy-vorticity feedback (Figs. 5e–f) and AO-related eddy forcing (Figs. 6e–f) are much weaker than the amplitudes in the observations; the simulated amplitudes at a zero-pentad lead time are only ∼33% of observed values.

These results indicate that BCC_AGCM2.2 reproduces the positive feedback of synoptic eddy activity on the AO/NAO mode during winter reasonably well. However, the amplitude of such feedbacks is much weaker than the observed amplitudes, which is attributed mainly to the systematic weakening of storm track activity in the model. The question thus arises as to the corresponding impact of the weakened amplitudes of storm track activity on the skill of BCC_AGCM2.2 in predicting subseasonal variability of the AO/NAO during winter.

The temporal evolution of the AO/NAO can be described as a first-order autoregressive process (Feldstein, 2000). Hence, the damping rate of the amplitude is positively related to the autocorrelation coefficient observed in the time series. To compare the damping rate of the daily AO/NAO index between the hindcasts and observations, we plotted the logarithm of autocorrelation coefficient of the daily AO and NAO indices as a function of lead time, in observations and in the BCC_AGCM2.2 hindcasts during winter (Fig. 7). Fig. 7 clearly shows that the autocorrelation coefficient of the daily AO and NAO indices decreases more rapidly with time in BCC_AGCM2.2 than in observations after approximately day 12. This indicates that weakening of storm track activity and AO/NAO-related synoptic eddy feedback in BCC_AGCM2.2 may result in more rapid damping of the daily AO/NAO index during winter in the hindcasts than in observations.

4.3. Impact of the stratosphere on the prediction skill of BCC_AGCM2.2 with respect to the AO/NAO

The downward propagation of stratospheric polar vortex anomalies provides an important source of predictability of surface climate variability during winter, when the stratosphere and troposphere are dynamically coupled (Baldwin et al., 2003; Maycock et al., 2011; Sigmond et al., 2013; Tripathi et al., 2015). As observed in Fig. 8, the correlation skill of BCC_AGCM2.2 in predicting the daily SPV index during winter is ∼17 days, which is higher than the persistence prediction skill of observations (∼14 days). Also, the dynamical skill of the model at predicting the daily SPV index is significantly higher than that of the daily AO/NAO index (Fig. 2a); this may help to improve the predictability of surface AO/NAO at subseasonal timescales.

Fig. 9 compares the prediction skill of BCC_AGCM2.2 with respect to the daily AO index for a case in which SPV signals are strong in the initial conditions during winter (i.e., the amplitude of the SPV index is greater than 1) as compared with a case in which SPV signals are weak during winter (i.e., the amplitude of the SPV index is less than 1). We found that the correlation skill with respect to the daily AO index in the former case (red line in Fig. 9) is ∼1 day higher than that for the latter case (blue line in Fig. 9) after ∼7 days. The difference in the skill of the model in predicting the daily NAO index in these two cases is fairly weak, which is most likely because the pattern of SLP anomalies associated with the SPV index closely resembles a hemispheric-scale annular pattern (Fig. 10). Specifically, the northern lobe of the SPV-related dipole is primarily

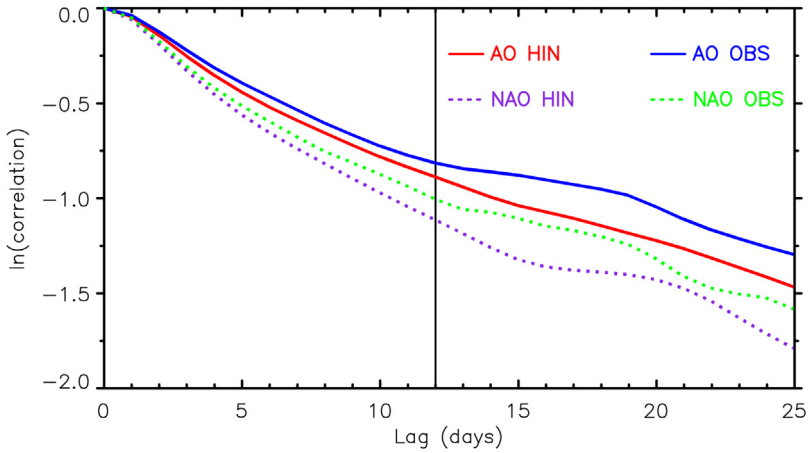

Fig. 7. Logarithm of the autocorrelation of the daily AO and NAO indices as a function of lead time during winter. The red (purple) line indicates the autocorrelation of the daily AO (NAO) index for the model hindcasts, and the blue (green) line indicates the autocorrelation of the daily AO (NAO) index for the observations.

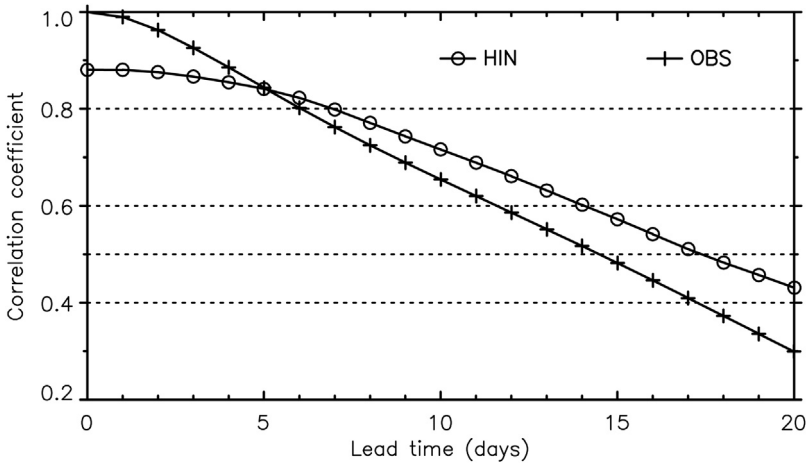

Fig. 8. Forecast skill of observations (crosses) and model hindcasts (circles) with respect to the daily SPV index as a function of lead time during winter.

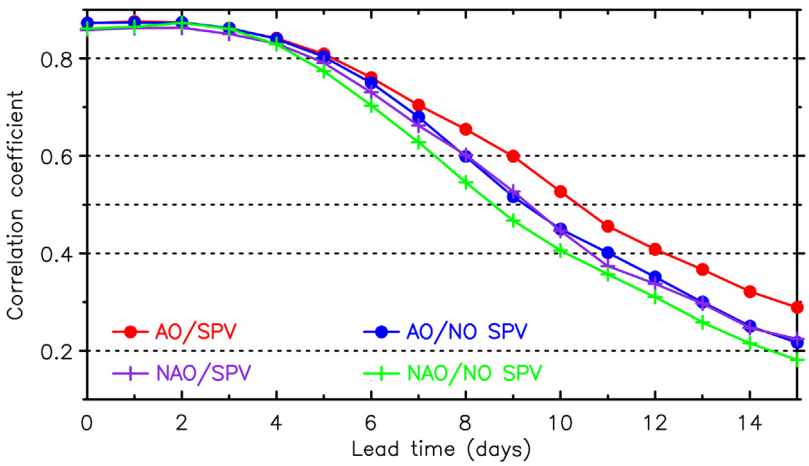

Fig. 9. Forecast skill of model hindcasts with respect to daily AO and NAO indices as a function of lead time for all cases in which a strong SPV signal exists in the initial conditions (amplitude of the SPV index greater than 1; AO/SPV and NAO/SPV) and in which a weak SPV signal exists in the initial conditions (amplitude of the SPV index less than 1; AO/NO SPV and NAO/NO SPV) during winter.

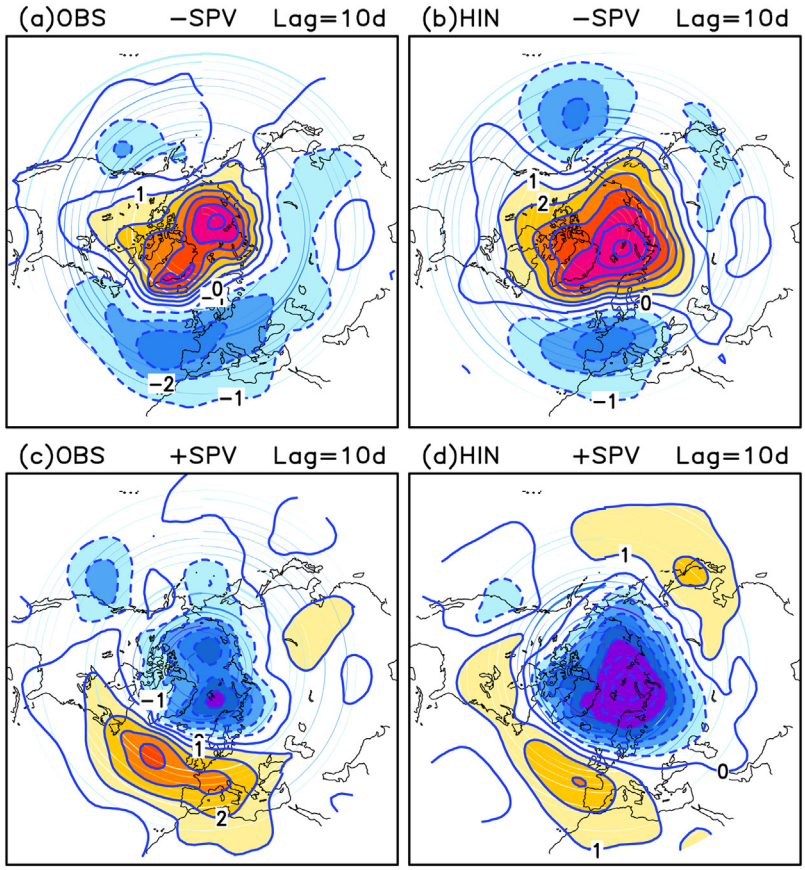

Fig. 10. Ten-day lagged composites of sea level pressure anomalies for the negative SPV phase in (a) observations and (b) model hindcasts. (c–d) As in (a–b), but for the positive SPV phase.

centered at the North Pole in both observations and in the BCC_AGCM2.2 hindcast (Fig. 10), whereas the northern lobe of the observed NAO pattern is centered over Iceland and adjacent regions (Fig. 3e).

To further examine the downward propagation of the SPV signal from the stratosphere to the troposphere, Fig. 11 displays the temporal evolution of regional-averaged (60°N–70°N, 0°E–360°E) zonal wind anomalies with respect to the phase of the SPV index during winter. When the SPV index is in a negative (positive) phase, easterly (westerly) anomalies propagate from the stratosphere to the upper troposphere in both observations and BCC_AGCM2.2, concurrent with easterly (westerly) anomalies near the surface. However, the amplitude of the zonal wind anomalies in BCC_AGCM2.2 appears to be stronger than that in observations.

Fig. 12 shows the correlations between the winter-mean SPV index and zonal-mean zonal wind anomalies in the extratropics. Also, the result shows that the relationship between the SPV and tropospheric zonal wind anomalies is overestimated in BCC_AGCM2.2 as compared with observations. Moreover, the correlation coefficient between the observed winter-mean SPV and AO indices is 0.58, while the correlation coefficient between the predicted SPV and AO indices is >0.80 (Table 1). These results indicate that stratosphere–troposphere coupling is overestimated in BCC_AGCM2.2 during winter.

A previous study suggested that the model's performance in simulating stratosphere–troposphere coupling is related to stratospheric climatology in the model (Peings et al., 2012). As observed in Fig. 13, the climatological winter-mean of the zonal-mean zonal wind is clearly stronger in BCC_AGCM2.2 than in observations in the extratropical stratosphere. Furthermore, in BCC_AGCM2.2 the simulated polar night jet core is displaced northward relative to observations. Sensitivity experiments from Peings et al. (2012) demonstrate that a more northerly position and greater intensity of the polar night jet might lead to more intense stratosphere–troposphere coupling in the extratropics. This suggests that the overestimation of stratosphere–troposphere coupling in BCC_AGCM2.2 is one possible reason for the poor representation of the mean state of the stratospheric polar vortex in the model.

5. Discussion and conclusions

The subseasonal variability and predictability of the AO/NAO were evaluated using a full set of hindcasts generated from BCC_AGCM2.2 and observations from the ERA-Interim Reanalysis dataset during 1983–2013. The results show that

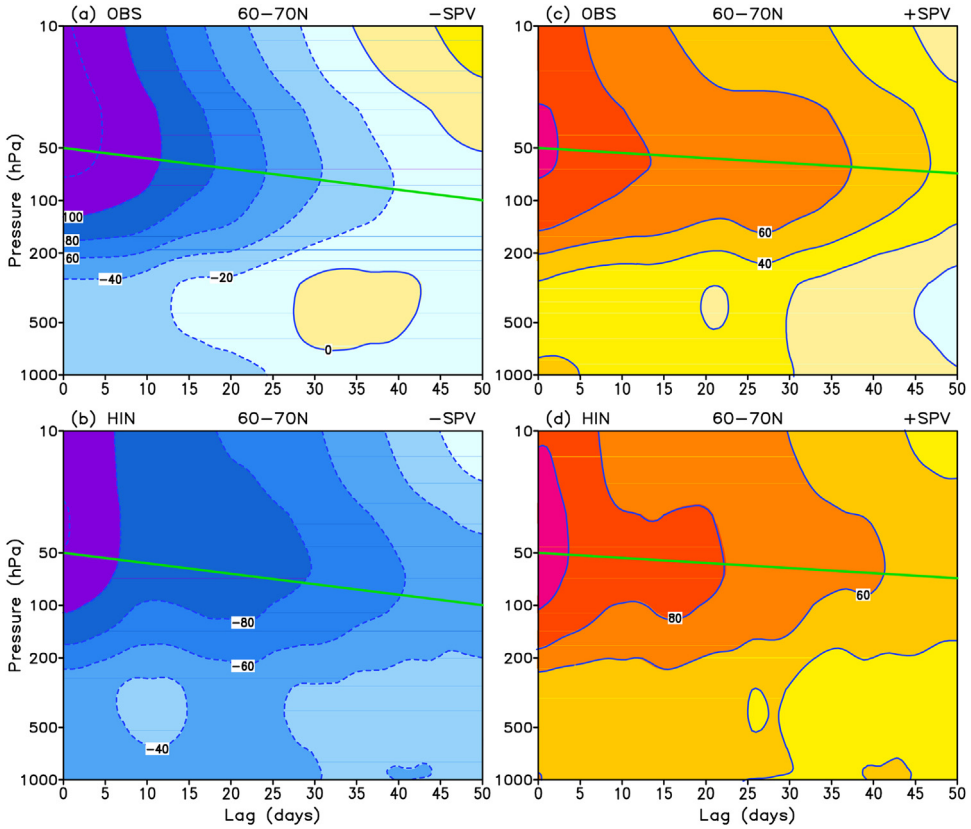

Fig. 11. Composites of the time–height evolution of normalized zonal-mean zonal wind anomalies averaged over 60°N–70°N for the negative SPV phase in (a) observations (b) and model hindcasts. (c–d) As in (a–b), but for the positive SPV phase.

the predictability of the NAO index is nearly equivalent to that of the AO index in both BCC_AGCM2.2 and observations at subseasonal timescales. The monthly mean AO/NAO index exhibits seasonally varying predictability, with the highest predictability during winter (December–March) and lowest predictability during autumn (August–November). As compared with the persistence skill of observations, BCC_AGCM2.2 is relatively skillful at predicting the monthly mean AO/NAO index at a one-pentad lead time for all winter months, and at a lead time of up to two pentads in December and January. During winter, BCC_AGCM2.2 exhibits an acceptable skill at predicting the daily AO/NAO index of ~9 days, which is higher than the persistence prediction skill of observations of ~4 days.

To examine the potential sources of subseasonal predictability of the AO/NAO in BCC_AGCM2.2, we further diagnosed the model's performance in reproducing the spatial patterns of the AO/NAO and related mechanisms for maintaining the patterns involving synoptic eddy feedback during winter. We found that the AO/NAO patterns simulated by BCC_AGCM2.2 closely resemble the observed patterns. The model also performs well in reproducing the positive feedback of synoptic eddies on the low-frequency mode, but clearly underestimates the amplitude of eddy forcing, as compared with observations. Such an underestimation is attributed primarily to systematic weakening of storm track activity intensity in the model, and may have a contribution to the more rapid damping of the simulated AO/NAO indices than the observed indices. One possible reason for the more rapid damping of the simulated atmospheric circulation may be related to the uncoupling of the atmosphere and ocean in BCC_AGCM2.2, in which a persistent sea surface temperature is prescribed initially.

We also investigated the impact of stratospheric initial conditions on the skill of BCC_AGCM2.2 at predicting subseasonal AO/NAO variability during winter. As compared with the case in which the stratospheric polar vortex is normal in the initial conditions, the correlation skill of BCC_AGCM2.2 at predicting the daily AO/NAO index is greater in the case in which the stratospheric polar vortex is strongly disturbed from its normal state in the initial conditions. Moreover, the skill of the model at predicting the stratospheric polar vortex is evidently greater than its prediction of the AO/NAO indices. These results imply that accurate representation of stratospheric circulation in the initial conditions may help to improve the predictability of the surface AO/NAO at subseasonal timescales during winter (Sigmond et al., 2013; Tripathi et al., 2015). However, we found that troposphere–stratosphere coupling is clearly stronger in BCC_AGCM2.2 than in observations, which may be partly related to a more northward position and greater intensity of the polar night jet in the model. Some previous studies have suggested that climate models with higher upper boundaries tend to show better performance in simulating stratospheric climatology and variability, as compared with models with lower upper boundaries (Charlton-Perez et al.,

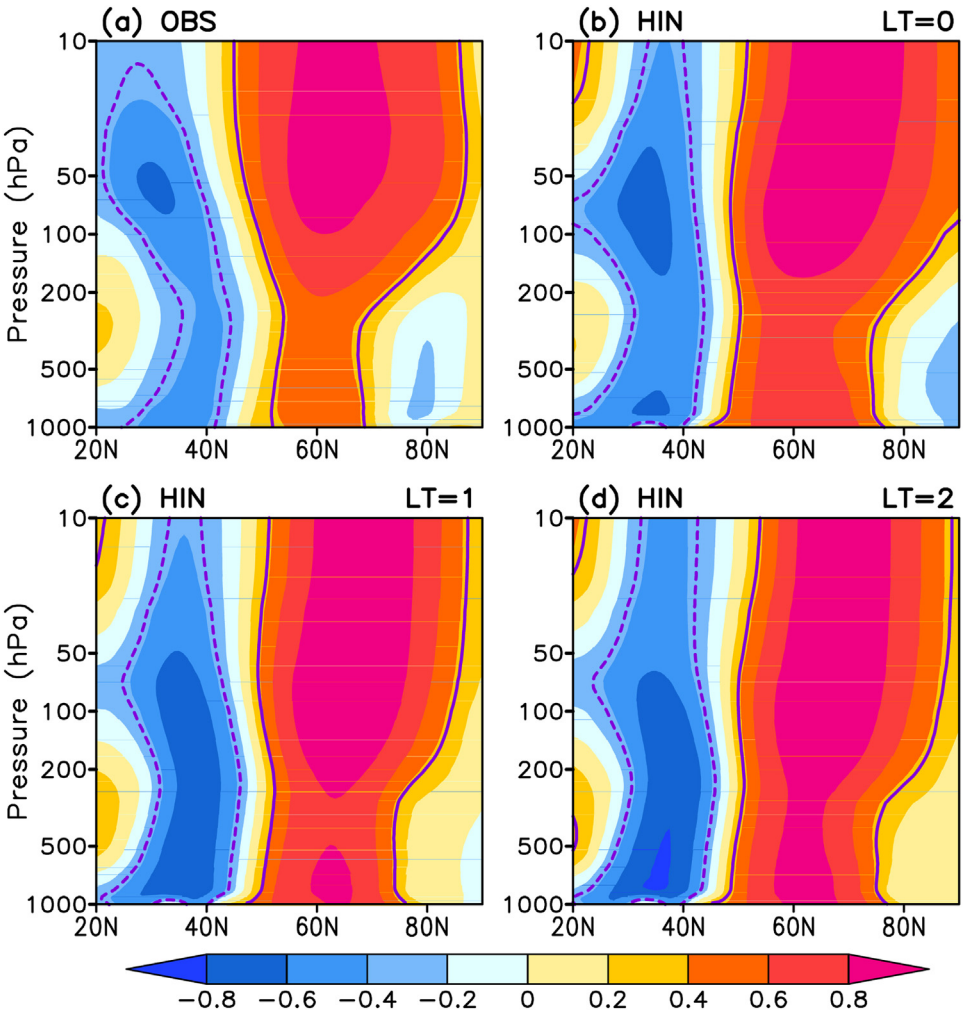

Fig. 12. Correlation between the SPV index and zonal-mean zonal wind anomalies in (a) observations and (b–d) model hindcasts at lead times of zero to two pentads. Regions inside the contours indicate significance at the 95% confidence level.

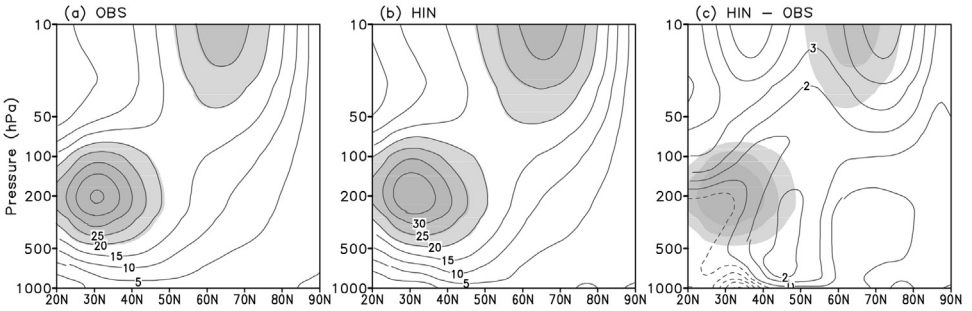

Fig. 13. Climatological mean of the zonal-mean zonal wind (unit: $m\,s^{-1}$) in (a) observations and (b) model hindcasts at a zero-pentad lead time, and (c) the difference between observations and hindcasts. Regions with zonal wind speeds greater than $20\,m\,s^{-1}$ are shaded. Shading in (c) is the same as in (a).

2013; Osprey et al., 2013). The low upper boundary of BCC_AGCM2.2 (below the stratopause) might contribute to the poor performance of the model in simulating stratospheric climatology, as shown in our results.

Although BCC_AGCM2.2 skillfully predicts subseasonal AO/NAO variability during winter, as compared with the persistence predictions of observations, the skill score is still much lower than that of the state-of-the-art ECMWF dynamical forecast system (see Figs. 7 and 8 in Vitart, 2014). We suggest that improvements in the simulation of storm track activity, synoptic eddy feedback, and troposphere–stratosphere coupling in the extratropical Northern Hemisphere could help to improve the skill of the model at predicting subseasonal AO/NAO variability during winter. However, sensitivity experiments

and detailed comparison between simulations of BCC_AGCM2.2 and other state-of-the-art climate model (such as ECMWF model) are still needed to fully diagnose deficiencies in BCC_AGCM2.2. Additionally, MJO signals in the initial conditions may influence the AO/NAO through atmospheric teleconnection (Zhou and Miller, 2005; Cassou, 2008), and thus provide a source of predictability of subseasonal AO/NAO variability (Vitart, 2014). Though BCC_AGCM2.2 shows a relatively good performance in the MJO simulations (Zhao et al., 2014, 2015), the impact of MJO on the predictability of subseasonal AO/NAO variability in this model should be addressed in the future.

Acknowledgements

This work was jointly supported by the 973 Program of China under Grant 2015CB453203, the China meteorological special project under Grant GYHY201406022, the China National Science Foundation under Grants 41205058 and 41375062, and also partly supported by the UK–China Research & Innovation Partnership Fund through the Met Office Climate Science for Service Partnership (CSSP) China as part of the Newton Fund. We thank Dr. Fei–Fei Jin for helpful discussions on an earlier version of this manuscript. The authors are grateful to two anonymous reviewers for their insightful comments to improve the quality of the paper.

References

Arribas, A., et al., 2011. The GloSea4 ensemble prediction system for seasonal forecasting. Mon. Weather Rev. 139, 1891–1910.
Baldwin, M.P., Dunkerton, T.J., 2001. Stratospheric harbingers of anomalous weather regimes. Science 294, 581–584.
Baldwin, M., Stephenson, D.B., Thompson, D.W.J., Dunkerton, T.J., Charlton, A.J., O'Neill, A., 2003. Stratospheric memory and skill of extended-range weather forecasts. Science 301, 636–640.
Branstator, G., 1992. The maintenance of low-frequency atmospheric anomalies. J Atmos. Sci. 49, 1924–1945.
Cassou, C., 2008. Intraseasonal interaction between the Madden–Julian oscillation and the north atlantic oscillation. Nature 455, 523–527.
Chang, E.K.M., Fu, Y., 2002. Interdecadal variations in Northern Hemisphere winter storm track intensity. J. Clim. 15, 642–658.
Charlton-Perez, A.J., et al., 2013. On the lack of stratospheric dynamical variability in low-top versions of the CMIP5 models. J. Geophys. Res. Atmos. 118, 2494–2505.
Dee, D.P., et al., 2011. The ERA-Interim reanalysis: configuration and performance of the data assimilation system. Q. J. R. Meteorol. Soc. 137, 553–597.
Doblas-Reyes, F.J., Pavan, V., Stephenson, D.B., 2003. The skill of multimodel seasonal forecasts of the wintertime North Atlantic Oscillation. Clim. Dyn. 21, 501–514.
Feldstein, S.B., 2000. The timescale, power spectra, and climate noise properties of teleconnection patterns. J. Clim. 13, 4430–4440.
Gerber, E.P., et al., 2012. Assessing and understanding the impact of stratospheric dynamics and variability on the earth system. Bull. Am. Met. Soc. 93, 845–859.
Hurrell, J.W., Kushnir, Y., Visbeck, M., Ottersen, G., 2003. An overview of the North Atlantic Oscillation, in The North Atlantic Oscillation: Climatic significance and environmental impact. Geophys. Monogr. Ser. 134, edited by J. W. Hurrell et al., pp. 1–35, AGU, Washington, D.C.
Hurrell, J.W., 1995. Transient eddy forcing of the rotational flow during Northern winter. J. Atmos. Sci. 52, 2286–2301.
Jin, F.-F., Pan, L.-L., Watanabe, M., 2006a. Dynamics of synoptic eddy and low-frequency flow interaction: part I: a linear closure. J. Atmos. Sci. 63, 1677–1694.
Jin, F.-F., Pan, L.-L., Watanabe, M., 2006b. Dynamics of synoptic eddy and low-frequency flow interaction: part II: a theory for low-frequency modes. J. Atmos. Sci. 63, 1695–1708.
Johansson, Å., 2007. Prediction skill of the NAO and PNA from daily to seasonal time scales. J. Clim. 20, 1957–1975.
Kalnay, E., et al., 1996. The NCEP/NCAR 40–year reanalysis project. Bull. Am. Meteorol. Soc. 77, 437–472.
Kang, I.-S., Kug, J.-S., Lim, M.-J., Choi, D.-H., 2011. Impact of transient eddies on extratropical seasonal-mean predictability in DEMETER models. Clim. Dyn. 37, 509–519.
Kang, D., Lee, M.-I., Im, J., Kim, D., Kim, H.-M., Kang, H.-S., Schubert, S.D., Arribas, A., MacLachlan, C., 2014. Prediction of the Arctic Oscillation in boreal winter by dynamical seasonal forecasting systems. Geophys. Res. Lett. 41, 3577–3585.
Kim, H.-M., Webster, P.J., Curry, J.A., 2012. Seasonal prediction skill of ECMWF System 4 and NCEP CFSv2 retrospective forecast for the Northern Hemisphere winter. Clim. Dyn. 39, 2957–2973.
Kug, J.-S., Jin, F.-F., Park, J.-H., Ren, H.-L., Kang, I.-S., 2010. A general rule for synoptic-eddy feedback onto low-frequency flow. Clim. Dyn. 35, 1011–1026.
L'Heureux, M.L., Higgins, R.W., 2008. Boreal winter links between the Madden–Julian oscillation and the Arctic Oscillation. J. Clim. 21, 3040–3050.
Lau, N.-C., Holopainen, E.O., 1984. Transient eddy forcing of the time-mean flow as indentified by geopotential tendencies. J. Atmos. Sci. 41, 313–328.
Lau, N.-C., Nath, M.J., 1991. Variability of the baroclinic and barotropic transient eddy forcing associated with monthly changes in the midlatitude storm tracks. J. Atmos. Sci. 48, 2589–2613.
Li, J., Wang, J.X.L., 2003. A new North Atlantic Oscillation index and its variability. Adv. Atmos. Sci. 20, 661–676.
Lin, H., Brunet, G., Derome, J., 2009. An observed connection between the North Atlantic Oscillation and the Madden–Julian oscillation. J. Clim. 22, 364–380.
Lorenz, D.J., Hartmann, D.L., 2003. Eddy-zonal flow feedback in the Northern Hemisphere. J. Clim. 16, 1212–1227.
Müller, W., Appenzeller, A.C., Schar, C., 2005. Probabilistic seasonal prediction of the winter North Atlantic Oscillation and its impact on near surface temperature. Clim. Dyn. 24, 213–226.
Maycock, A.C., Keeley, S.P.E., Charlton-Perez, A.J., Doblas-Reyes, F.J., 2011. Stratospheric circulation in seasonal forecasting models: implications for seasonal prediction. Clim. Dyn. 36, 309–321.
Norton, W.A., 2003. Sensitivity of Northern Hemisphere surface climate to simulation of the stratospheric polar vortex. Geophys. Res. Lett. 30, 1627.
Osprey, S.M., Gray, L.J., Hardiman, S.C., Butchart, N., Hinton, T.J., 2013. Stratospheric variability in twentieth-century CMIP5 simulations of the Met Office climate model: high top versus low top. J. Clim. 26, 1595–1606.
Peings, Y., Saint-Martin, D., Douville, H., 2012. A numerical sensitivity study of the influence of Siberian snow on the northern annular mode. J. Clim. 25, 592–607.
Qian, Z.L., Wang, H.J., Sun, J.Q., 2011. The hindcast of winter and spring Arctic and Antarctic Oscillation with the coupled climate models. Acta. Meteorol. Sin. 25, 340–354.
Ren, H.-L., Jin, F.-F., Kug, J.-S., Zhao, J.-X., Park, J., 2009. A kinematic mechanism for positive feedback between synoptic eddies and NAO. Geophys. Res. Lett. 36, L11709.
Ren, H.-L., Jin, F.-F., Kug, J.-S., Gao, L., 2011. Transformed eddy-PV flux and positive synoptic eddy feedback onto low-frequency flow. Clim. Dyn. 36, 2357–2370.
Ren, H.-L., Jin, F.-F., Gao, L., 2012. Anatomy of synoptic Eddy-NAO interaction through eddy structure decomposition. J. Atmos. Sci. 69, 2171–2191.

Ren, H.-L., Jin, F.-F., Kug, J.-S., 2014. Eddy-induced growth rate of low-frequency variability and its mid- to late winter suppression in the Northern Hemisphere. J. Atmos. Sci. 71, 2281–2298.
Reynolds, R.W., Rayner, N.A., Smith, T.M., Stokes, D.C., Wang, W., 2002. An improved in situ and satellite SST analysis for climate. J. Clim. 15, 1609–1625.
Riddle, E.E., Butler, A.H., Furtado, J.C., Cohen, J.L., Kumar, A., 2013. CFSv2 ensemble prediction of the wintertime Arctic Oscillation. Clim. Dyn. 41, 1099–1116.
Robertson, A.W., 2001. Influence of ocean-atmosphere interaction on the Arctic Oscillation in two general circulation models. J. Clim. 14, 3240–3254.
Scaife, A.A., Knight, J.R., Vallis, G.K., Folland, C.K., 2005. A stratospheric influence on the winter NAO and North Atlantic surface climate. Geophys. Res. Lett. 32, L18715.
Scaife, A.A., et al., 2014. Skillful long-range prediction of European and North American winters. Geophys. Res. Lett. 41, 2514–2519.
Sigmond, M., Scinocca, J.F., Kharin, V.V., Shepherd, T.G., 2013. Enhanced seasonal forecast skill following stratospheric sudden warmings. Nat. Geosci. 6, 98–102.
Sun, J., Ahn, J.-B., 2015. Dynamical seasonal predictability of the Arctic Oscillation using a CGCM. Int. J. Climatol. 35, 1342–1353.
Tan, G.-R., Jin, F.-F., Ren, H.-L., Sun, Z.-B., 2014. The role of eddy feedback in the excitation of NAO. Meteorol. Appl. 21, 768–776.
Thompson, D.W.J., Wallace, J.M., 1998. The Arctic oscillation signature in the wintertime geopotential height and temperature fields. Geophys. Res. Lett. 25, 1297–1300.
Thompson, D.W.J., Wallace, J.M., 2000. Annular modes in the extratropical circulation. Part I month-to-month variability. J. Clim. 13, 1000–1016.
Thompson, D.W.J., Wallace, J.M., 2001. Regional climate impacts of the Northern Hemisphere annular mode. Science 293, 85–89.
Tripathi, O.P., Charlton-Perez, A., Sigmond, M., Vitart, F., 2015. Enhanced long-range forecast skill in boreal winter following stratospheric strong vortex conditions. Environ. Res. Lett. 10, 104007.
Vitart, F., 2014. Evolution of ECMWF sub-seasonal forecast skill scores. Q.J.R. Meteorol. Soc. 140, 1889–1899.
Wallace, J.M., 2000. North Atlantic oscillation/annular mode: two paradigms—one phenomenon. Q. J.R Meteor. Soc. 126, 791–805.
Wang, L., Chen, W., 2010. Downward Arctic Oscillation signal associated with moderate weak stratospheric polar vortex and the cold December 2009. Geophys. Res. Lett. 37, L09707.
Wu, T.W., et al., 2014. An overview of BCC climate system model development and application for climate change studies. J. Meteor. Res. 28, 34–56.
Yamazaki, K., Shinya, Y., 1999. Analysis of the arctic oscillation simulated by AGCM. J. Meterol. Soc. Japan 77, 1287–1298.
Zhao, C., Zhou, T., Song, L., Ren, H., 2014. The boreal summer intraseasonal oscillation simulated by 4 Chinese AGCMs participated in CMIP5 project. Adv. Atm. Sci. 31, 1167–1180.
Zhao, C., Ren, H., Song, L., Wu, J., 2015. Madden-Julian oscillation simulated in BCC climate models. Dyn. Atmos. Oceans 72, 88–101.
Zhou, S., Miller, A.J., 2005. The interaction of the Madden-Julian Oscillation and the Arctic oscillation. J. Clim. 18, 143–159.
Zuo, J., Ren, H.-L., Li, W., 2015. Contrasting impacts of the Arctic Oscillation on surface air temperature anomalies in Southern China between early and middle-to-late winter. J. Clim. 28, 4015–4026.